Capacity of fillet welded joints made of ultra high strength steel

Björk T., Toivonen J., Nykänen T
Laboratory of Fatigue and Strength
Lappeenranta University of Technology
P.O. Box 20. FIN-53851 Lappeenranta. Finland

Ruukki is a metal expert you can rely on all the way, whenever you need metal based materials, components, systems or total solutions. We constantly develop our product range and operating models to match your needs.

- **Abstract**

The ultimate load-bearing capacity of typical fillet welded joints made of ultra-high-strength steel (UHSS) S960 has been investigated. The aim of the work has been to assess the validity of current design rules for UHSS and possibly define new design criteria. Experimental testing and nonlinear finite element analysis (FEA) was applied to define the capacity of fillet welded joints. Joint geometries and material properties were measured for both filler and base materials. In comparison with current design rules, the experimental results showed that the fillet welded joints had adequate load carrying capacity presuming that weld quality is proper. Load carrying capacities and rupture modes in welds defined by FEA agreed quite well with experimental results. The experimental deformation capacities of some joints were found to be critical, but the capacities can be improved by use of undermatched filler metals. Heat input control is essential in fabrica-tion of welded connections made of UHSS and thus an additional failure criteria should be con-sidered in design codes due to the softening effect in HAZ.

- **Indroduction**

Using of high strength steels for weight critical construction is one way to save energy and to minimize the carbon foot print in future. Weight critical structures are typical of all moving constructions like carriers frame, lifting and hoisting devices but also many predominantly statically loaded structures, where the weight can impor-tant due to transportation, assembly and maintenance. Lighter construction means generally thinner wall thick-nesses and thus smaller welds meaning savings also for fabrication. Independent on the nature of the service load (static or fatigue) the joints must be designed always for static loading.

Several reports are published concerning the static strength of welded joints fabricated from conventional structural steel with yield strength equal or less than 460 MPa. For this strength cate-gory of steels the design of welded connections is properly guided in relevant design codes like Eurocode 3 [1]. Eurocode 3 part 1-12 extends the design rules to cover the steel grades up to S700 and allows also the use of undermatched filler

metals [2]. Kuhlman, Günter, Collin & al. have investi-gated the ultimate strength of filled welded joints made steel grades in this category [3, 4, 5]. However, there is no generally accepted design rules or published results available concerning the static strength of steel grades over 700 MPa, which in this paper is set to be the lower limit strength value for UHSS.

The main goal of this study is to investigate the valida-tion of the current design rules for welded joints which are fabricated from direct quenched (untempered) ultra high strength steel S960. These design rules concern the assessment of throat thickness and other dimensions for filled welds. The validity will be proved by experimental testing and applying of nonlinear finite element analy-sis (FEA). The experimental test results are compared with capacities calculated according to Eurocode 3. The paper is based on the Master's Thesis by Joe Toivonen, which deals the subject in more details [6].

- **2. Material properties**

The chemical composition and mechanical properties of the base and filler materials are seen in Table 1 and 2. If available, both nominal and measured values for the used materials are pre-sented.

The strength of the welded joint depends on the region of the weld as illustrated in Figure 1.
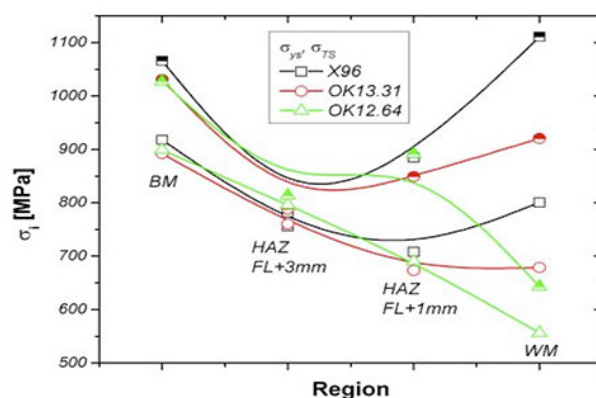

Figure 1. Strengths of filler metals in terms of joint region [7]

- **Chemical composition of S960** *Table 1*

	C	Mn	Si	P	S	Ti
nominal (max)	0.11	1.20	0.25	0.02	0.01	0.07
measured	0.089	1.04	0.20	0.012	0.004	0.03

Mechanical properties of materials   *Table 2*

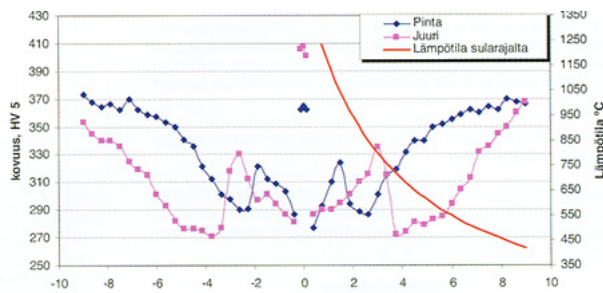| group	material code		f_y MPa	f_u MPa	A5 %	KV [J]
base material (BM)	S960	nominal	960	1000	7	50 (-40 °C)
		measured	1014	1076	12.5	
filler metal = weld (WM)	X96	nominal	930	980	14	40 (-40 °C)
		measured	990	1245		
	12.64	nominal	470	500 [2]	26	70 (-30°C)
		measured	580	690		
	13.31	nominal	850	890	18	50 (-30°C)
		measured	790	915		

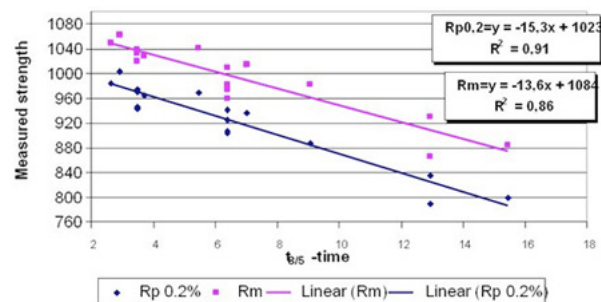Figure 2. Hardness (HV5) – distributions in a butt weld of S960 & X96 (0 = centreline of the weld) [8]

Figure 3. Strength of S960 versus cooling time t8/5 [9]

For matched filler metals the weakest strength appears in HAZ but for undermatched electrodes in the weld itself. According to the IIW recommendation the carbon equivalent can be calculated using the following formula

$$CEV = C + \frac{Mn}{6} + \frac{Cr + Mo + V}{5} + \frac{Ni + Cu}{15},$$

which obtains in this case the value C_{ekv} = 0.51. A typical hardness distribution for a butt weld of S960 with X96 filler metal is seen in Figure 2.

The weldability of the steel is good and no preheating (welding in elevated temperature) is needed for the plate thickness up to 8 mm. On the contrary, the material is prone for softening effect due the heat input and thus the heat input by welding should be limited to minimum level. Opposite to conventional structural steels there seems to be no upper limit for cooling rate and the best mechanical properties for direct quenched steel S960 are reached, if the $t_{8/5}$-times could be less than 10 s as illustrated in Figure 3. By using GMAW process (MAG) for joining of the current plate thicknesses of 8 mm, the optimal cooling rate is difficult to reach and small heat input increase also the risk of fusion failure by welding.

● **3. Experimental tests**
3.1 Joint types and parameters
A typical drawing for test joint fabrication is illustrated in Figure 4. For each joint the heat input is controlled according welding process specification (WPS) prepared for each joint. The lap joints were welded using a narrow gap between the parallel plates in order to avoid contact with plates and thus eliminating the friction effect on the joint behaviour.

The used fully-mechanised welding process ensured to minimize the variation of throat thickness and penetration for each weld. In order to obtain theoretically correct throat thicknesses for studied joints the penetration in the root of the weld was adjusted as illustrated in Figure 5. This is a delicate requirement consider the used process (GMAW-process) and its susceptibility for incomplete fusion. The throat thicknesses were measured using manual calibre and laser distance transducer.

The studied joints are load carrying (L-. T-. LT- and X-series) and non-load carrying (X0-series) joints as illustrated in Tables 3-7. Each joint type includes several
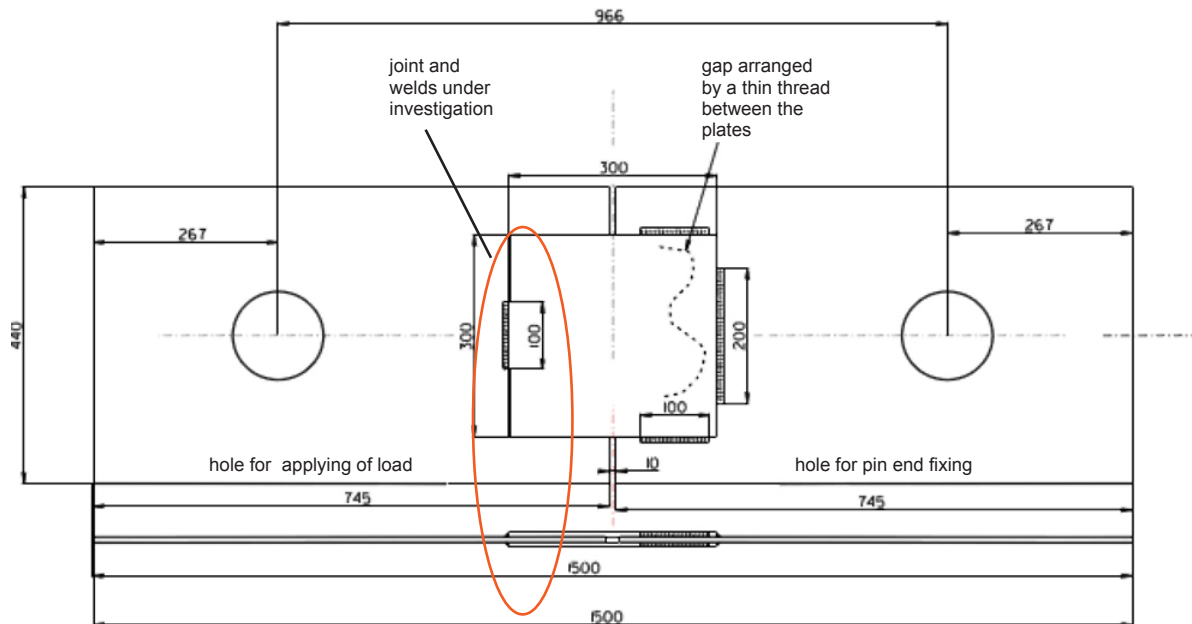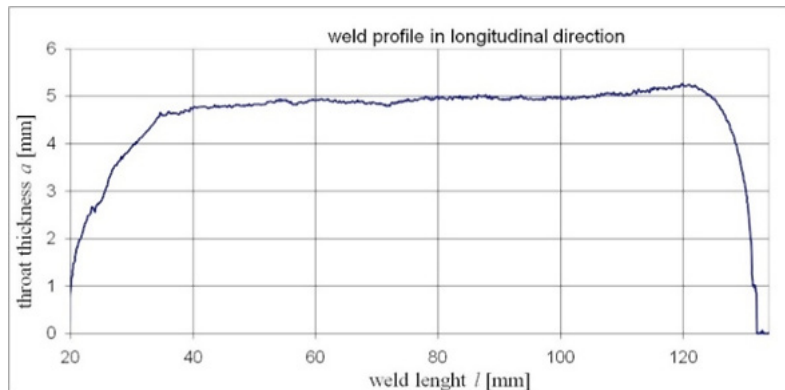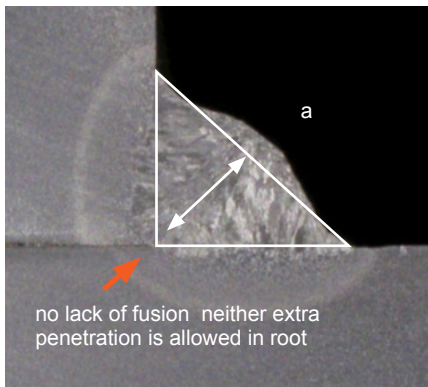
Figure 4. A typical test specimen (T-series)

Figure 5. A fillet weld of test specimens. transverse view and longitudinal distribution for *a*.

parameters such as type of the filler metal, length l and throat thickness a of the welds. When possible the start and end parts of the fillet weld were machined away in order to keep the effective length unambiguous. In the cases this tooling was not applicable the effective throat thickness was defined my measuring the profile of the throat thickness along the weld length as illustrated in Figure 5. The value from manual throat thickness calibre was applied as reference dimension for fixing the profile high.

Longitudinal loaded cruciform joint (L-series) *Table 3*
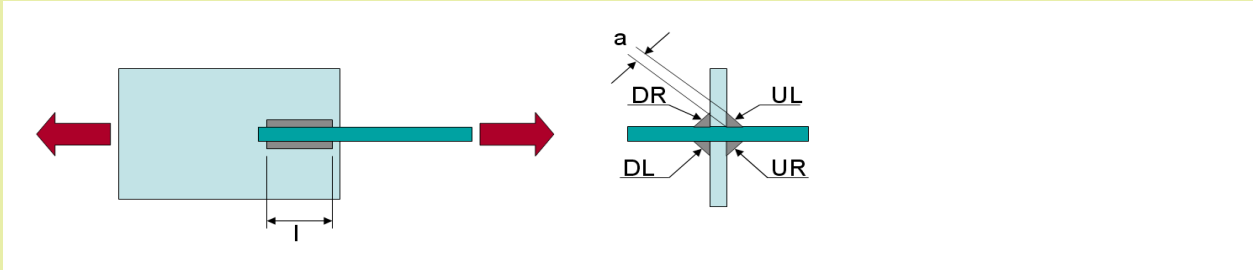
ID	filler metal	UL		UR		DL		DR	
		l	*a*	*l*	*a*	*l*	*a*	*l*	*a*
L1_1	X96	109.10	2.96	108.06	3.31	108.98	3.57	109.58	3.25
L2	X96	113.04	4.60	112.60	5.14	112.26	4.78	116.36	4.54
L3	12.51	110.55	3.30	114.14	3.30	110.80	3.08	110.98	3.38
L4	12.51	110.84	4.48	113.56	4.55	113.38	4.35	112.60	4.58
L5	X96	109.78	3.64	109.52	3.67	110.54	3.09	110.02	3.38
L6	X96	112.14	4.59	112.40	4.68	110.54	4.35	111.36	4.73
L7	X96	112.10	2.94	112.40	3.46	113.08	2.76	110.02	3.33
L10	13.31	108.94	3.14	109.62	2.98	113.38	3.13	109.52	3.21
L11	13.31	110.10	4.33	109.28	5.30	110.09	4.78	111.92	4.41
L12_1	X96	–	–	612.8	4.49	–	–	614.3	4.10
L13	X96	–	–	408.2	3.81	–	–	401.4	3.94
L14	X96	–	–	310.0	4.52	–	–	314.0	4.4
L15	X96	–	–	209.4	4.27	–	–	206.1	4.45
L16	X96	–	–	163.76	4.15	–	–	159.38	4.44

Transverse load carrying lap joint (T-series) *Table 4*
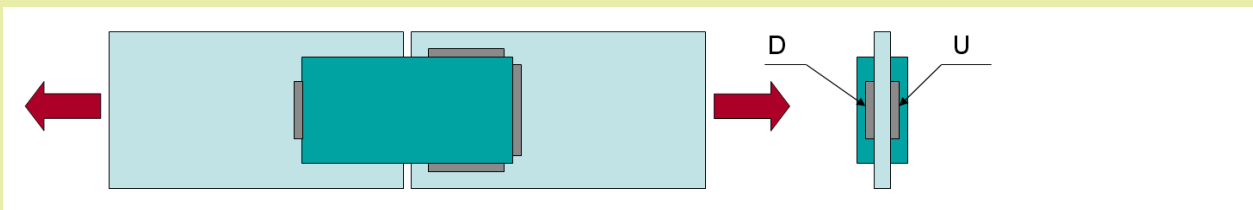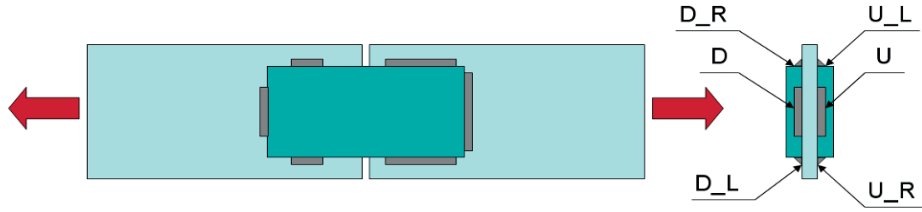
ID	filler metal	U		D	
		l	*a*	*l*	*a*
T1	X96	100.3	3.01	100.3	3.00
T2_2	X96	100.0	4.64	100.0	5.00
T3	12.51	100.0	3.00	100.0	2.85
T4_1	12.51	98.5	5.04	98.5	4.83
T5_1	X96	100.2	3.18	100.15	3.10
T6	X96	100.0	5.44	99.95	5.55
T7	X96	100.4	2.86	100.4	2.85
T10	13.31	101.0	2.87	101.0	2.90
T11	13.31	100.0	4.27	100.0	4.31

Transverse and longitudinal load carrying lap joint (LT-series) *Table 5*
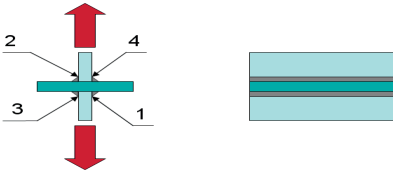
ID	filler metal	U		U_L		U_R		D		D_L		D_R	
		l	a	l	a	l	a	l	a	l	a	l	a
LT1	X96	100.2	2.98	80.8	2.91	66.78	2.80	100.0	2.85	68.9	2.75	68.7	2.88
LT2	X96	100.2	5.46	71.18	4.74	72.06	4.69	100.15	5.28	73.0	4.86	72.36	4.18
LT3_1	12.51	100.2	3.09	70.59	2.81	71.34	2.96	100.4	3.06	69.54	3.02	71.0	2.95
LT4	12.51	100.1	5.17	69.14	5.07	72.52	4.52	99.9	5.56	75.92	5.02	67.82	4.51
LT5	X96	100.15	3.03	71.04	2.74	69.64	2.89	100.1	2.91	67.68	2.59	65.42	2.95
LT6	X96	100.2	4.73	71.54	4.33	73.54	4.38	100.15	5.13	77.0	3.88	71.54	4.64
LT7_2*	X96	99.95	3.07	204.8	3.14	204.3	3.16	99.95	3.17	204.2	3.03	210.8	2.96
LT8*	X96	100.25	4.11	306.0	4.05	303.8	3.97	100.1	3.89	307.0	3.77	308.6	3.96

Load carrying transverse cruciform joint (X-series) *Table 6*

ID	filler metal	1		2		3		4	
		l	a	l	a	l	a	l	a
X1_1	X96	99.6	3.4	99.6	3.4	99.6	3.2	99.6	3.3
X2_1	X96	86.38	3.82	86.72	4.11	85.20	3.80	87.80	4.30
X3_1	X96	69.68	4.40	74.70	4.37	70.70	4.57	74.68	4.80
X4_1	X96	60.94	4.68	61.96	4.96	59.46	4.79	63.44	5.04
X5	12.51	99.9	4.9	99.6	5.4	99.9	5.2	99.6	4.9
X6	12.51	61.20	4.70	61.42	4.45	60.68	4.33	62.14	4.68
X7_1	X96	99.6	3.1	99.5	3.0	99.6	3.0	99.5	3.2
X8_1	X96	71.42	4.32	73.98	4.44	71.52	4.45	73.58	4.14
X9_1	X96	85.24	2.73	84.82	3.03	84.24	3.03	85.76	3.16
X12	13.31	99.7	3.2	99.7	3.2	99.7	3.0	99.7	2.5
X13	13.31	71.78	3.71	71.92	3.76	66.56	4.21	70.12	4.19

● Non load carrying transverse cruciform joint (X0-series)   *Table 7*
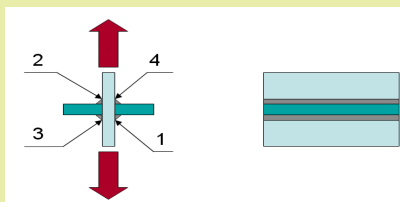
ID	filler metal	1		2		3		4	
		l	a	l	a	l	a	l	a
X01	X96	99.5	3.5	99.55	3.3	99.5	3.2	99.55	3.5
X02	X96	99.7	4.6	99.9	4.6	99.7	4.4	99.9	4.4
X04	X96	98.8	5.2	98.8	5.2	98.8	5.4	98.8	5.4
X05*	X96	99.0	6.5	99.0	5.6	99.0	6.2	99.0	5.6
X06	X96	98.7	3.6	98.7	3.2	98.7	3.5	98.7	3.6
X07	X96	99.1	5.3	99.2	4.8	99.1	5.2	99.2	4.2
X010	X96	99.3	5.4	99.5	5.5	99.3	5.0	99.5	5.3

3.2 Test set up

A typical test set up with boundary conditions and apply of force is seen in Figure 6. Quasi-static loading was increased by displacement control until failure took place. For LT-series the displacements were measured separately for longitudinal and transverse welds. For L-series the transducers were fixed in the middle and in the end of the longitudinal weld. The displacement transducers were fixed on the weld toes in order to define the deformations in the weld only and to eliminate the displacements in the base plates. In all the cases also the total deformation of the specimen was measured by the movement of the hydraulic jack in the loading rig.

Figure 6. Test set up for a LT-test

3.3 Experimental test results

A typical load-displacement-curve for a test specimen is seen in Figure 7. The total (δt) and plastic (δp) displacements are defined for the critical welds. Also the applied load F versus total dis-placement on the specimen (δF) were recorded in tests. The results from the experimental tests are presented in Table 8.

● 4. Finite element analysis
4.1 Modelling of specimens

The nonlinear finite element analysis (FEA) was applied to evaluate the joint behaviour and to compare the results with experimental tests. Modelling and post-pro-

cessing was carried out with Femap 10.0.2 software. NX Nastran 6 was used as a solver and calculations were based on non-linear Newton-Raphson method [10].

Four different load carrying joint types (L, T, LT and X) from experimental test series were analysed. The measured minor values of joint geometry were used for modelling the chosen test specimens: L15, L16, T1, LT2 and X1_1. Symmetry was utilized to simplify the models and Hex-Mesh solid-elements with eight nodes were used for meshing. A typical FE-model for weld geometry is plotted in Figure 8.
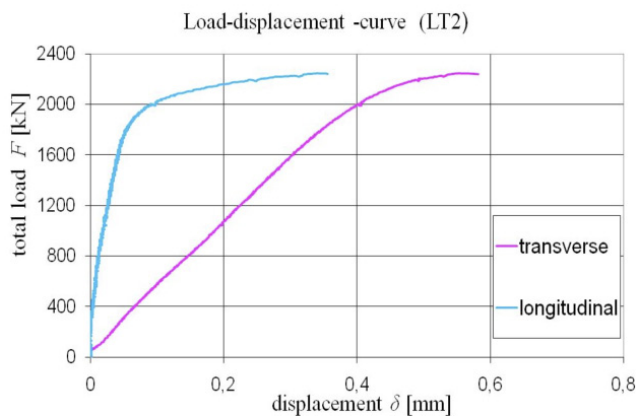

Figure 7. Load –displacement -curve for transverse and longitudinal welds of a test specimen
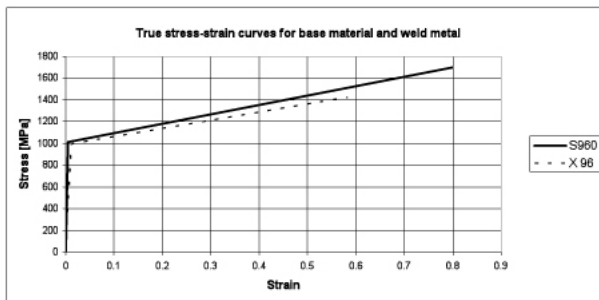

Figure 8. A part of FEA-model for a cruciform L-joint

Figure 9. The used true-stress-strain-curve for base and filler materials
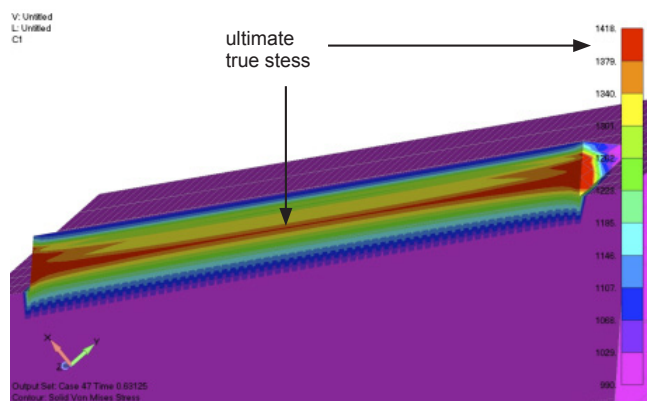
Figure 11. Von Mises stresses in weld

Figure 10. A typical load-displacement curve from FEA (test LT2)

• Experimental test results

Table 8

ID	δ_p [mm]	δ_t [mm]	δ_F [mm]	Fu [kN]	place of fracture W= weld BL = base plate FLF =fusion line failure	note! LOF= lack of fusion
L1_1	0.1	0.3	0.1	494	W	LOF
L2	2.3	2.6	5.0	1115	W	
L3	1.4	1.5	1.8	721	W	
L4	4.2	4.3	4.3	932	W	
L7	0.7	0.9	1.5	1094	W	
L10	0.2	0.4	0.2	920	W	
L11	1.4	1.5	1.8	1070	W	
L12_1	0.3	0.4	6.0	3087	W and BL	
L13	0.2	0.3	1.6	1900	W	
L14	0.3	0.4	5.2	1640	W	
L15	0.9	1.0	1.4	1235	W	
L16	1.1	1.2	1.5	941	W	
T1	0.3	0.5	0.3	797	W	
T2_1b	0.4	1.0	1.8	1304	W	
T3	0.3	0.7	0.3	631	W	
T4_1	0.7	0.8	0.8	904	W	
T7	0.0	0.3	0.0	830	W	
T10	0.1	0.5	0.1	587	W	
T11	0.1	0.4	0.1	1042	W	
X1_1	0.2	0.3	0.3	640	W, FLF	
X2_1	0.8	1.0	0.3	640	W, FLF	
X3_1	0.4	0.5	0.3	474	W, FLF	
X4_1	0.2	0.3	0.3	420	W, FLF	
X5	0.9	1.0	1.0	600	W	
X6	0.3	0.4	0.3	303	W	
X9_1	0.3	0.4	0.3	530	W, FLF	
X12	0.2	0.2	0.2	560	W, FLF	
X13	0.1	0.3	0.2	470	W, FLF	
X01	0.0	0.1	14.0	874	HAZ	
X02	0.1	0.3	10.6	874	HAZ	
X04	0.8	0.9	0.8	769	W	
X05	0.1	0.2	14.2	872	HAZ	
X010	0.8	0.9	1.8	840	W	

ID	δ_{pL} [mm]	δ_{pT} [mm]	δ_{tL} [mm]	δtT [mm]	δ_F [mm]	Fu [kN]		
LT1	0.1	0.1	0.2	0.4	0.2	1122	W	
LT2	0.4	0.2	0.4	0.6	2.0	2250	W	
LT3_1	1.3	0.9	1.4	1.2	1.0	874	W	
LT4	1.0	1.0	1.0	1.2	4.7	1638	W	
LT7	0.1	0.6	0.1	1.9	0.4	1495	W	LOF
LT8	0.1	0.3	0.1	0.4	7.0	4560	HAZ	

Deformation and load carrying capacities from FEA *Table 9*

ID	δ$_p$ [mm]	δ$_t$ [mm]	F$_u$ [kN]
L15	0,8	1,0	1270
L16	1,2	1,3	1170
T1	0,7	0,8	1020
LT2	L:1,1 T:0,3	L:1,2 T:0,4	2400
X1_1	1,4	1,5	900

5.Discussion

The capacity of the fillet weld can de calculated according to Eurocode 3 using the stress component in the critical plane of weld throat thickness as illustrated in Figure 12.

Using von Mises stress criteria the theoretical strength of the fillet weld joint can be calculated

$$\sigma_w = \sqrt{\sigma_\perp^2 + 3(\tau_\perp^2 + \tau_\parallel^2)} = \frac{f_u}{\beta_w \gamma_{M2}}$$

Where the σ and τ are stress components according to Figure 12, f_u is tensile strength of the base material and β_w is the ratio for tensile strengths of weld and base material and $_{\gamma M2}$ safety factor = 1.25. Eurocode 3, part 1 – 12 allows the use of undermatched filler material and this is assumed to valid also for the current steel S960. In consequence the capacity of the joint can be calculated by replacing the tensile strength of the base material by tensile strength of the filler metal feu. The required joint load bearing capacities F can be defined for joints of L-series,

$$F = \frac{f_u}{\sqrt{3}\beta_w \gamma_{M2}} \sum_i a_i l_i$$

and for joint of T and X-series

$$F = \frac{f_u}{\sqrt{2}\beta_w \gamma_{M2}} \sum_i a_i l_i$$

and for joint of LT-series

$$F = \frac{f_u}{\sqrt{2}\beta_w \gamma_{M2}} \sum_{i,trans.} a_i l_i + \frac{f_u}{\sqrt{3}\beta_w \gamma_{M2}} \sum_{j,longit.} a_j l_j$$
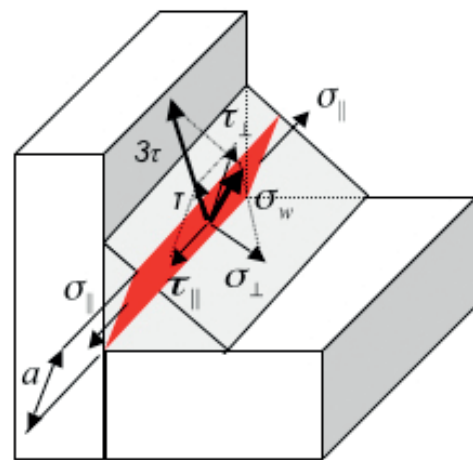

Figure 12. Stress components in the plane of throat thickness

For non load carrying of X0- series where the softening can take place next the weld

$$F = \frac{f_u t b}{\gamma_{M2}}$$

where f_u is the tensile strength either of the base material or the softened HAZ whereas t and b are the plate thickness and width, respectively. Comparison between experimental and theoretical load bearing capacities of the joints are seen in Figure 13. The theoretical capacities of joints are calculated using measured tensile strength (engineering values) either of filler metal or base material, depending on the failure place. The nominal ultimate strength is nominal value of the base material except in the case of undermacthed filler metal, where the nominal strength is defined according Eurode 3, part 1 – 12. The black columns relate the safety level available by designers and the grey columns refer to the real safety level of the applied procedure. The safety levels are depending on the joint type: the experimental test results of T-series prove the highest extra strength whereas the tested joint capacities of L- and X-series match quite well with theoretical evaluation
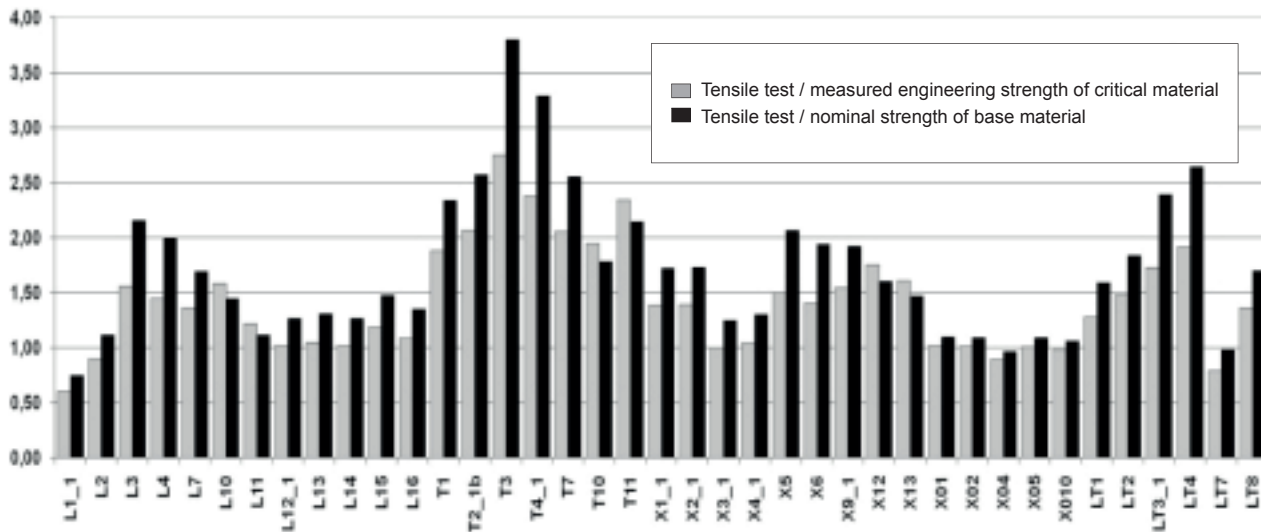
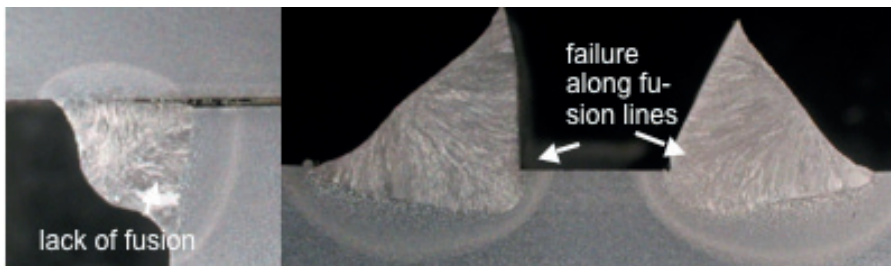Figure 13. Comparison of tests results with theoretical results

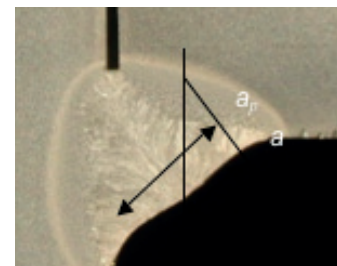Figure 14. Fracture plane including lack of fusion

Figure 15. Extra penetration in root side of weld increase the load carrying capacity of the joint

In the joints where the load carrying capacities from experimental tests are below the theoretically defined values appeared locally lack of fusion in welds or failure in fusion line. The previous one can be find out by means of visual inspection of welds before or after the test but the later one after test as illustrated in Figure 14.

In the case the load bearing capacity of the joint exceeded the theoretical value considerable, one reason is the extra penetration in the root of the weld found in some joints as seen in Figure 15.

The more accurate comparison between tested and calculated results can be carried out after the areas of failure surfaces are measured. This procedure is quite arduous but it will consider the effects involving in lack of fusion and extra penetration.

Typically the failure took place in the angle of 45 degrees in welds subjected to pure shear stresses in

longitudinal direction of weld (L and LT-series) agreeing with the theoretical assump-tion. However, in the joints subjected to transverse loading (T, LT and X-series) rupture followed either the fusion line of the weld or fail-ure plane formed an angle $\alpha \approx 20$ degrees in the weld. The experimental findings agreed well with results from nonlinear FEA, as illustrated in Figure 16, where also the distribution of the plastic strain in weld are plotted for comparison.

The load carrying capacities depend on length-throat thickness-ratio (l/a) of the weld in longi-tudinal direction loaded joint are seen in Figure 17. It can be noticed that the capacity will be de-crease if l/a-ratio exceed the value of 50, which can thus set to be allowable limit without strength reduction in calculations. More tests will be needed in order to define the reduction factor for l/a > 50.
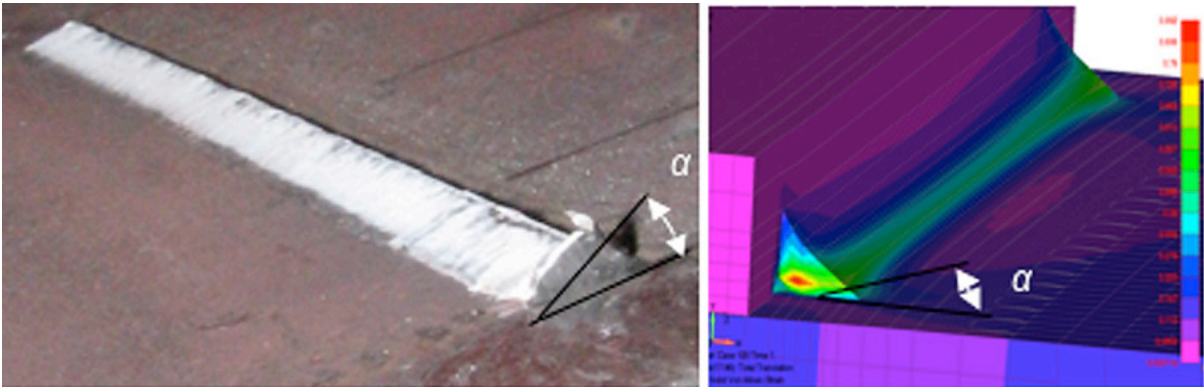
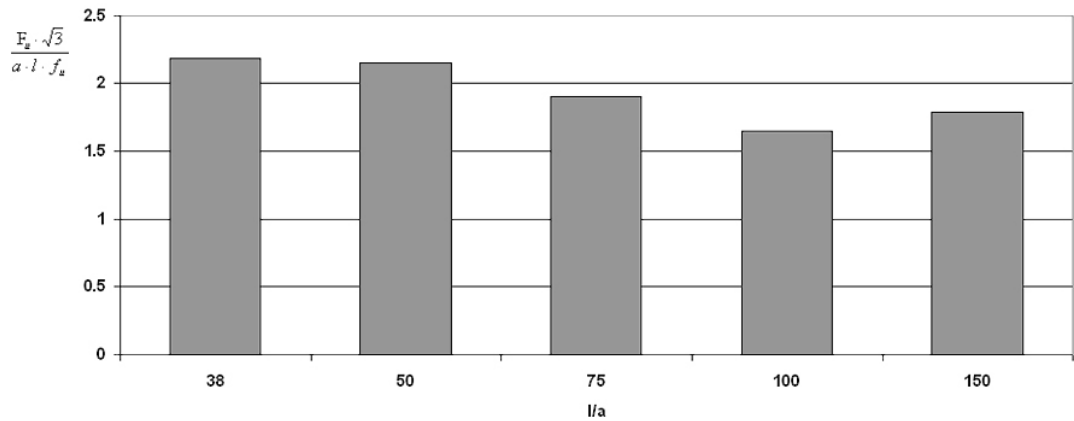Figure 16. Fracture planes from experimental tests with comparison of FEA-results (T-series)

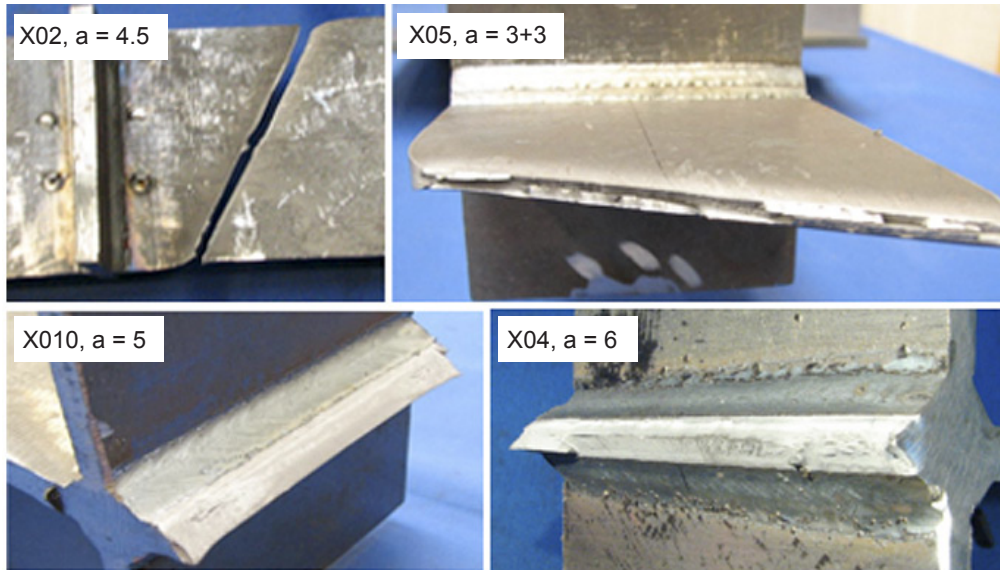Figure 17. Effect of the l/a-ratio on the joint strength

Figure 18. Failure modes in non load carrying joints (X0-series)

The failure and capacity of non load carrying joints (X0-series) seems to be depend on the heat input due to welding. If the heat input is low, the softening is local and it has no effect on the capacity of the joint and the failure take place outside the joint (typically tilting in angle of 30 degrees as illustrated in Figure 18). If the heat input will be increased the softened width/plate thickness-ratio increases and the critical ratio (> 0.2) can be exceeded and consequently failure takes place in HAZ next to weld. This phenomena is not necessary to consider when using the conventional steels but it typically accompanied welded joints made of aluminium alloy. For the X0-joint with 8 mm plate thickness the limit heat input value seems to 4.5 mm in terms of throat thickness. The failure took place in HAZ in joints with 5 mm and 6 mm throat thickness but in base plate outside the HAZ, if the throat thickness was less than 4.5 mm or if it was larger but executed by multi pass welding.

From the Table 8 it can bee seen, that the plastic deformation capacity (δ_p) of the joint is remarkably less than what can be expected with fillet welded joints made of conventional structural steel ($f_y \leq 460$ MPa), where $\sigma_p \approx$

0.5 mm in transverse direction and 1.0 mm in longitudinal directions are typical requirements. However, some overall plasticity in the weld occured which is an essential criterien concerning the basic assumptions for the applied design approach of welded joints. In generally the longitudinal fillet welds have a little bit more plastic deformation capacity compared to transversely loaded welds. Using an undermatched filler metals better plastic deforma-tion capacity can be reached. Hence it is recommend to use undermatched electrodes with increased throat thickness for fillet welds loaded in transverse direction. Although the used filler material do not enable to reach the degree of plastic deformation typical of conventional structural steels they do not seems to prevent to reach the ultimate load carrying capacity of joint. This proves the plastic deformation capacity seems to be adequate for this type of joint geometries and loading conditions and in all cases the failure mode was ductile in tests executed in room temperature.

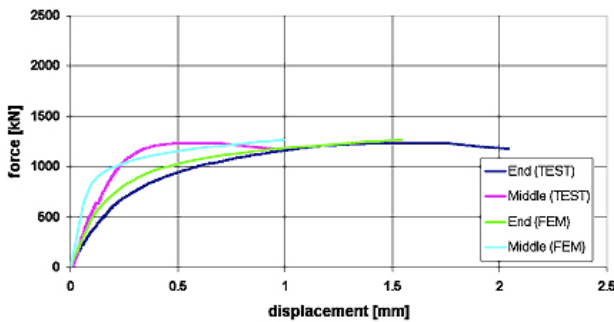In Figures 19 – 22 are seen some comparison of load-displacement behaviours with experimental tests and FE-analyses.

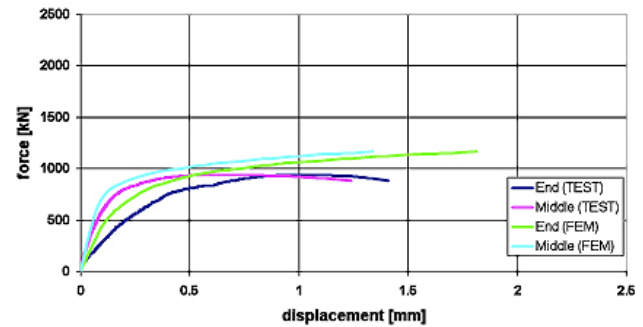Figure 19. Comparison of F-δ-curves between experimental test and FEA for L15

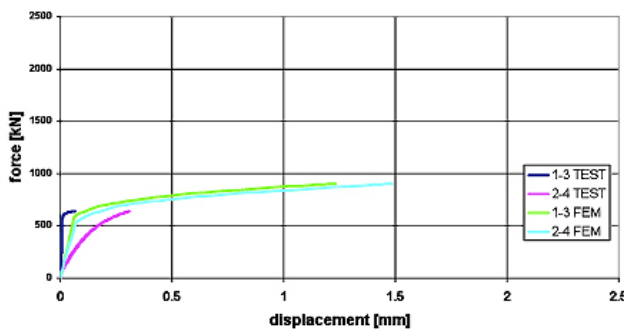Figure 20. Comparison of F-δ-curves between experimental test and FEA for L16

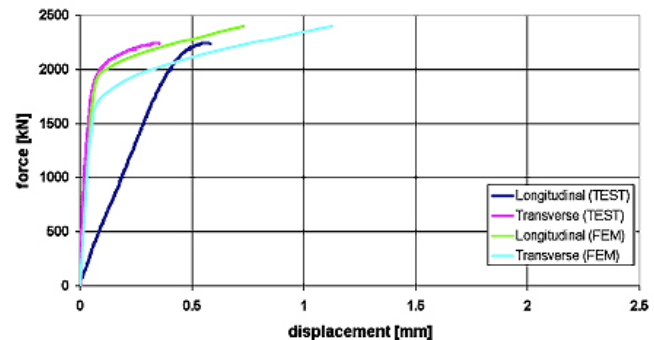Figure 21. Comparison of F-δ-curves between experimental test and FEA for X1_1

Figure 22. Comparison of F-δ-curves between experimental test and FEA for LT2

Generally the load carrying capacities from FEA match quite well with experimental results. However, the calculated displacement values can distinguish considerable from test results, as can be seen also from results in Tables 8 and 9. The difference can exist because the used classical continuum mechanics approach does predict properly the strain based rupture. Also all kind of unsymmetrical behaviour of joint can cause errors in displacement values measured in experi-mental tests.

6. Conclusions

Experimental test were carried out for fillet welded joints weld made of ultra high strength S960 steel and the capacities were compared with results from nonlinear FEA. The following conclu-sions can be drawn out:

- load carrying capacity of the studied joints seems to be evaluated using the current design rules [1, 2]
- deformation capacity was remarkable lower compared the capacities of conventional struc-tural steel up to f_y ≤ 460 MPa
- failure mode was ductile rupture for all in room temperature tested joint
- using of undermatched filler material can be improved the deformation capacity of filled welds
- FEA predicted the ultimate capacity and failure path quite well but not the ultimate deformation capacity
- heat input is essential due to softening effect in HAZ and it should be considered (like in alu-minium structures) if the critical heat input limits can not be followed
- additional analyses involved in statistical evaluation of current results, fracture path and effective fracture area (penetration-flaws) corrections, softening of HAZ and joint design is going on
- future testing and calculation concerning capacities of hybrid joints. undermatched electrodes an low ambient temperatures will be needed and executed in near future

7. References

1. EN 1993-1-8. Eurocode 3: Design of steel struc-tures. part 1-8: Design of joints, 2005
2. prEN 1993-1-12. Eurocode 3. Additional rules for extension of the 1993 up to grades S700, 2006
3. Kuhlmann U., Günther H-P., Rasche C., High – strength steel fillet welded connections. Steel Con-struction. Design and Research. Volume 1, 2008
4. Günther H-P., Hildebrand J., Rasche C., Versch C., Wudtke I., Kuhlmann U., Vormwald M., Werner F., Welded connections of high strength steels for build-ing industry. IIW XV-1315-09, 2009
5. Collin P., Johansson B., Design of welds in high strength steel. 4th European conference on steel and composite structures. Maastricht 2005
6. Toivonen. J., Ultralujasta teräksestä valmistetun liitoksen pienahitsin staattinen lujuus. Mas-ter's The-sis, Lappeenranta University of Technology, 2010
7. Nevasmaa P., Karjalainen-Roikonen P., Laukkanen A., Kuoppla J., Ultralujan, suorakarkais-tun Optim 960 QC ohutlevyteräksen lujuus- ja sitkeyskäyttäy-tyminen. Hitsaustekniikka 3/2010
8. Pirinen J., Pulssi-MAG hitsauksen optimointi ultra-lujille rakenneteräksille. Master's Thesis, Lappeen-ranta University of Technology, 2006
9. Karppi R., Leiviskä P., Keinoja parantaa ultralu-jan teräksen hitsausliitoksen staattista lujuut-ta ja väsymiskestävyyttä pulssi MAG hitsauksen avulla. Research report No VTT-R-04809-08. VTT, Espoo 2008
10. NX Nastran 6 Release Guide. Siemens Product Lifecycle Management Software Inc. 2008

For further information please contact:

Rautaruukki Corporation, Suolakivenkatu 1, FI-00810 Helsinki, Finland. Tel. +358 20 5911.
For further information please contact: info.metals@ruukki.com.